NANOSCALE GRAPHENE LITHOGRAPHY USING AN ATOMIC FORCE MICROSCOPE

K. Kumar and E.H. Yang

Department of Mechanical Engineering, Stevens Institute of Technology
Castle Point-on-Hudson, Hoboken, NJ 07030

ABSTRACT

In this work, we have systematically studied local oxidation lithography parameters using an Atomic Force Microscope (AFM) on graphene material. Graphene has recently been shown to have exceptional electrical properties which give it a niche in emerging nanoelectronics applications requiring quantum structures. The desktop AFM nanolithography technique has lately been shown [1-3] to fabricate graphitic nanodevices on the order of tens of nanometers. By applying an appropriate electric field between AFM tip and substrate in humid atmosphere, oxidation of the substrate occurs. Depending on such process parameters as applied voltage, tip speed, water meniscus length and humidity, the oxidation of the graphitic material enables the formation of insulating trenches to make various nanostructures. Using this optimized technique, we have oxidized nanometer-sized features on single and few layer graphene and graphite.

Keywords: Atomic Force Microscope, Graphene, Graphite, Lithography

1 INTRODUCTION

The Atomic Force Microscope (AFM) can be used to locally oxidize various materials to form nanometer size features [4-12]. Recently, the AFM has been used to etch graphene using the principle of local anodic oxidation. Application of an appropriate electric field between the tip and substrate dissociates the H2O molecules into H+ and OH-. The H+ ions rush towards the negatively charged tip and the OH- ions gather near the positively substrate. The oxygen reacts with the carbon in the graphitic material to form volatile or nonvolatile carbon oxides depending on the voltage applied. This oxidation, coupled with the x-y scanning capability of the AFM, allows for thin structure patterning ability. However, the effect of process parameters on feature size has not been completely studied. If the lithography parameters such as voltage, tip speed, meniscus length and humidity are well controlled, sub-100 nm patterning is possible on graphitic materials, especially for emerging nanoelectronics applications requiring quantum structures [13-18]. This technique can also be performed in the ambient environment, eliminating several fabrication steps, such as the poly(methyl methacrylate) (PMMA) processing required in conventional electron-beam lithography process. In order to establish this technique as a robust fabrication process, we have studied the process parameters and resulting feature size.

2 EXPERIMENTAL PROCEDURES

Graphite and few-layer graphene were mechanically exfoliated on silicon substrate. The samples were connected electrically to ground and placed in Pacific Nanotechnology NANO-I AFM system (Figure 1). Imaging was conducted in contact mode with a negatively biased sharp AFM tip. Patterns were drawn by the tip in this configuration with applied tip voltage running between -5V and -10V.

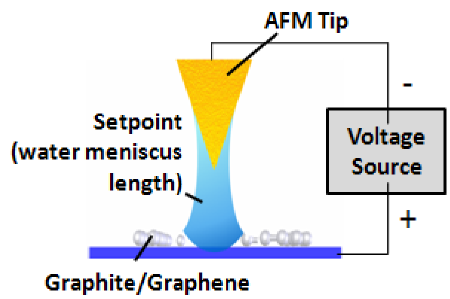

Figure 1: Schematic diagram of AFM oxidation lithography setup. An external voltage source is used to ground the graphite substrate and negatively bias the AFM tip. The water meniscus which naturally condenses around the tip and graphite facilitates local oxidation of the graphite upon application of the electric field.

Line patterns were created by scanning the AFM tip in a line across the substrate at a constant speed and setpoint while continuously applying a constant voltage. For parametric experiments, the water meniscus length (known as setpoint) was varied from 0.00 to 130 nm, and tip speed from 0.03 to 0.10 μm/s. Dot patterns were created by holding the tip steady above a point on the substrate and applying voltage for a specified period of time (holdtime). Holdtime, i.e. oxidation time per pixel is directly related to the tip speed, where one pixel is equal to the diameter of the AFM tip. The holdtime was varied from 250 ms to 500 ms. The resulting depth and width (diameter) of the lines (and dots) were measured and analyzed using the Pacific Nanotechnology Nanorule software.

3 RESULTS

Figures 2 shows AFM scans confirming the relationship between feature size and setpoint, voltage, and tip speed (or holdtime). In Figure 2a, as the tip is raised above the substrate from 35.5 nm to 59.2 nm in increments of 11.8 nm, the expected reduction in feature size is observed. Similarly, in Figure 2c, as the tip speed is varied from 0.03 μm/s to 0.10 μm/s in increments of 0.04 μm/s, feature size is observed to decrease.

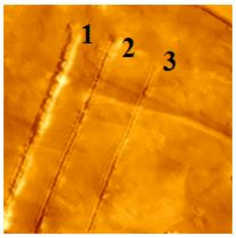

	Setpoint	Depth	Width
1	35.5	94.2	164
2	47.3	78.3	111
3	59.2	62.4	97.0

(a)

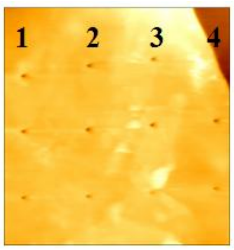

Voltage	1	2	3	4
-10	220	220	221	
-10	223	221	217	217
-8	179	171	164	169

(b)

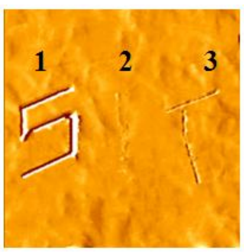

	Tip Speed	Depth	Width
1	0.03	58.5	224
2	0.1	1.24	117
3	0.07	6.60	146

(c)

Figure 2: (a) Line patterns showing variation of feature size with setpoint, (b) Dot pattern showing variation of feature size with voltage, (c) Line patterns showing variation of feature size with tip speed. AFM images of the local oxidation lithography process. Resulting feature sizes are shown in the tables next to each AFM scan. Experimental conditions: (a) voltage – -9V, tip speed – 0.03 μm/s, humidity - <20%, (b) setpoint – 0 nm, holdtime – 500 ms (0.06 μm/s), humidity - <20%, (c) voltage – -10V, setpoint – 0 nm, humidity - <20%.

Figure 2b shows dot patterns which illustrate the relationship between feature size and voltage. The expected trend of feature size (width) increasing with decreasing (negative) voltage is shown to hold. We find that on average, for the same voltage and setpoint and tip speed (holdtime), the dot patterns consistently produce larger feature sizes than the line patterns. We attribute this to the stability of the water meniscus during dot patterns. In the line scan, the tip is scanned across the hydrophobic graphite which can contribute to thinner line widths. However, in the dot patterns, the tip remains stationary above the graphite, which allows the meniscus to remain stabilized and of the same diameter throughout patterning.

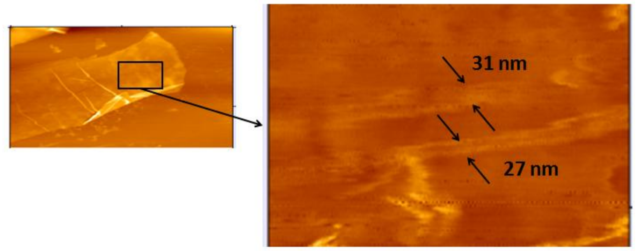

Figure 3: Experiment on few layer graphene. The minimum line width achieved was 27 nm under the following conditions: Voltage – -9.00V, setpoint – 20.0 nm, tip speed – 1.5 μm/s (20 ms holdtime).

Based on the results achieved from experiments similar to Figure 2, we optimized the process parameters to scan 31 nm and 27 nm width lines in few layer graphene (Figure 3). The voltage threshold found for etching was -8.00V. However, this value produced unreliable results unless dot patterns were fabricated. To etch these minimal line widths, -9.00V was used at a fast tip speed of 1.5 μm/s under high humidity conditions (>70% relative humidity) to ensure the stability of the water meniscus.

4 CONCLUSION

This experimental work on AFM tip-based oxidation lithography performed on graphite has illustrated the effect of parameter variation on the resulting feature size. Based on the results of this work, the minimum line width on few layer graphene was found to be 27 nm. Minimum graphite line width on graphite was found to be 55.0 nm. Further progress can be achieved by incorporating environmental control, which can indicate the effect of humidity on feature size. Forthcoming experiments will use this work's data to pattern single layer graphene into quantum nanoribbons for electron transport studies.

This work has been supported in part by the Air Force Office for Scientific Research (Award No. FA9550-08-1-0134) and the National Science Foundation (Grant No. NSF DGE-0742462).

REFERENCES

[1] L. Weng, L. Zhang, Y.P. Chen, and L. P. Rokhinson, "Atomic force microscope local oxidation nanolithography of graphene," Applied Physics Letters, vol.93, 093107, Sept. 2008.

[2] A.J.M. Giesbers, U. Zeitler, S. Neubeck, F. Freitag, K.S. Novoselov, J.C. Maan, "Nanolithography and manipulation of graphene using an atomic force microscope," Solid State Communications, vol. 147, pp. 366–369, July 2008.

[3] S. Masubuchi, M. Ono, K. Yoshida, K. Hirakawa, T. MacHida, "Fabrication of graphene nanoribbon by local anodic oxidation lithography using atomic

force microscope," Applied Physics Letters, vol. 94 (8), no. 082107, Feb. 2009.
[4] S.C. Minne, Ph. Flueckiger, H.T. Soh and C. F. Quate, "Atomic force microscope lithography using amorphous silicon as a resist and advances in parallel operation," Journal of Vacuum Science and Technology B: Microelectronics and Nanometer Structures, vol. 13, no. 3, pp. 1380-1385, May 1995.
[5] B. Irmer, M. Kehrle, H. Lorenz and J.P. Kotthaus, "Fabrication of Ti/TiOx tunneling barriers by tapping mode atomic force microscopy induced local oxidation," Applied Physics Letters, vol. 71, no. 12, pp.1733-1735, Sept. 1997.
[6] S. Myhra, "Tip-induced local anodic oxidation: nanolithography and nanobiotechnology," NanoBioTechnology, vol. 3, no. 3-4, pp. 212-222, Dec. 2007.
[7] R. Garcia, R.V. Martinez, and J. Martinez, "Nano-chemistry and scanning probe nanolithographies," Chemical Society Review, vol. 35, pp. 29-38, Nov. 2005.
[8] S. Bae, C. Han, M.S. Kim, C.C. Chung and H. Lee, "Atomic force microscope anodization lithography using pulsed bias voltage synchronized with resonance frequency of cantilever," Nanotechnology, vol. 16, no. 10, pp. 2082-2085, Aug. 2005.
[9] P. Cochran, "Nanometer-scale lithography using an atomic force microscope," NNIN REU Research Accomplishments, pp. 34-35, 2004.
[10] R. Held, T. Heinzel, P. Studerus, and K. Ensslin, "Nanolithography by local anodic oxidation of metal films using an atomic force microscope," Physica E, vol. 2, no. 1-4, pp. 748-752, Jul. 1998.
[11] P. Avouris, R. Martel, T. Hertel and R. Sandstrom, "AFM tip induced and current induced local oxidation of silicon and metal," Journal Applied Physics A: Materials Science & Processing, vol. 66, no. 1, pp. S659–S667, March 1998.
[12] M. Tello and R. García, "Nano-oxidation of silicon surfaces: Comparison of noncontact and contact AFM methods," Applied Physics Letters, vol. 79, no. 424, Jul. 2001.
[13] G.A. Steele, G. Götz, and L.P. Kouwenhoven, "Tunable few-electrodes double quantum dots and Klein tunnelling in ultra-clean carbon nanotubes," Nature Nanotechnology, vol. 4, pp. 363-367, Jun. 2009.
[14] S. Sapmaz, P. Jarillo-Herrero, Ya.M. Blanter, and H. S. J. van der Zant, "Coupling between electronic transport and longitudinal phonons in suspended nanotubes," New Journal of Physics, vol. 7, no. 1, pp. 243, Nov. 2005.
[15] S. Moriyama, T. Fuse, M. Suzuki, Y. Aoyagi, and K. Ishibashi, "Four-electron shell structures and an interacting two-electron system in carbon-nanotube quantum dots," Physical Review Letters, vol. 94, no. 18, 186806, May 2005.
[16] K. Ishibashi, S. Moriyama D. Tsuya, T. Fuse, and M. Suzuki, "Quantum-dot nanodevices with carbon nanotubes," Journal of Vacuum Science and Technology A, vol. 24, no. 4, pp. 1349-1355, Jun. 2006.
[17] A. Javey, J. Guo, Q. Wang, M. Lundstrom, and H. Dai, "Ballistic carbon nanotube field-effect transistors," Nature, vol. 424, no. 6949, pp. 654-657, Aug. 2003.
[18] W. Liang, M. Bockrath, D. Bozovic, J.H. Hafner, M. Tinkham, and H. Park, "Fabry-Perot interference in a nanotube electron waveguide," Nature, vol. 411, no. 6838, pp. 665-669, Jun. 2001.